1 **Validating Genome-Wide Association candidates through quantitative variation in nodulation**

2

3 Shaun J. Curtin[1†], Peter Tiffin[2†], Joseph Guhlin[2], Diana Trujillo[2], Liana Burghart[2], Paul Atkins[3], Nicholas J.

4 Baltes[3], Roxanne Denny[1], Daniel F. Voytas[3], Robert M. Stupar[4], and Nevin D. Young[1,2*]

5

6 [1]Department of Plant Pathology, University of Minnesota, St. Paul, MN, 55108. [2]Department of Plant

7 Biology, University of Minnesota, St. Paul, MN, 55108. [3]Department of Genetics, Cell Biology &

8 Development and Center for Genome Engineering, University of MN, Minneapolis, MN 55455.

9 [4]Department of Agronomy and Plant Genetics, University of Minnesota, St. Paul, MN, 55108. [†]These

10 authors contributed equally to this work. [*]email: neviny@umn.edu

11

12 ORCID ID: 0000-0002-9528-3335 (S.J.C.); 0000-0002-8836-2924 (R.M.S.); 0000-0001-6463-4772 (N.D.Y.)

13

14

15

16 One Sentence Summary:

17

18 GWAS combined with multiple mutagenesis technologies, including CRISPR/Cas9, were used to

19 functionally validate novel candidate genes contributing to phenotypic variation in symbiosis between

20 legume plants and rhizobial bacteria.

21

22

23

24

25 Author contributions:

26 S.J.C., P.T., N.D.Y., and R.M.S. designed research;

27 S.J.C., P.T., J.G., R.D., P.A., N.J.B., J.M., A.D.F., and D.F.V. performed research;

28 S.J.C, P.T., and N.D.Y. analyzed data;

29 S.J.C, P.T., and N.D.Y wrote the paper.

30

31 The authors declare no conflict of interest.

33 **Abstract**

34   Genome wide association (GWA) studies offer the opportunity to identify genes that contribute to

35 naturally occurring variation in quantitative traits. However, GWA relies exclusively on statistical

36 association, so functional validation is necessary to make strong claims about gene function. We used a

37 combination of gene-disruption platforms (Tnt1 retro-transposons, hairpin RNA-interference constructs,

38 and CRISPR/Cas9 nucleases) together with randomized, well-replicated experiments to evaluate the

39 function of genes that an earlier GWAS in *Medicago truncatula* had identified as candidates contributing

40 to variation in the symbiosis between legumes and rhizobia. We evaluated ten candidate genes found in

41 six clusters of strongly associated SNPs, selected on the basis of their strength of statistical association,

42 proximity to annotated gene models, and root or nodule expression. We found statistically significant

43 effects on nodule production for three candidate genes, each validated in two independent mutants.

44 Annotated functions of these three genes suggest their contributions to quantitative variation in nodule

45 production occur through processes not previously connected to nodulation, including phosphorous

46 supply and salicylic acid-related defense response. These results demonstrate the utility of GWA

47 combined with reverse mutagenesis technologies to discover and validate genes contributing to

48 naturally occurring variation in quantitative traits. The results highlight the potential for GWA to

49 complement forward genetics in identifying the genetic basis of ecologically and economically important

50 traits.

51

52

53

54   Genome wide association (GWA) studies offer the promise of identifying genes responsible for

55   quantitative trait variation in plants and animals (Mackay et al., 2009). Relative to forward genetic

56   screens, GWA has the potential to identify genes of much smaller phenotypic effect. Moreover, the

57   genes identified through GWA are expected to contribute to naturally occurring phenotypic variation. By

58   contrast, forward genetic screens identify genes that are functionally necessary but may or may not

59   contribute to natural variation. An important limitation of GWA analyses, however, is that the statistical

60   approach used to identify candidate genes is also expected to identify many false positives. Therefore,

61   functional validation of GWA candidates is essential for confirming the biological importance of the

62   identified genes (Ioannidis et al., 2009).

63   The symbiosis between legume plants and rhizobial bacteria is responsible for large inputs of

64   nitrogen into both natural and agricultural systems through symbiotic nitrogen fixation (Vance, 2001).

65   The ecological and economic importance of this symbiosis has made identifying its genetic basis an

66   important goal for plant biologists (Oldroyd et al., 2011). More than 30 plant genes that play central

67   roles in the formation and growth of plant nodules, the site of rhizobial symbiosis, and nitrogen fixation

68   have been identified (Popp and Ott, 2011; Pislariu et al., 2012). These genes were identified primarily

69   through forward genetic screens. In standard forward genetic screens, a mutant phenotype is identified

70   based on the effects seen within individual organisms, something that will bias these screens towards

71   detecting genes of large effect. Forward genetic screens are likely to miss genes of small phenotypic

72   effects, such as those that contribute to naturally occurring quantitative variation in nodulation

73   (Stanton-Geddes et al., 2013; Friesen et al., 2014). Identification of these genes of subtle effect will

74   provide a fuller understanding of the symbiosis between legumes and rhizobia, and may provide targets

75   for selection in important agronomic legumes.

76   Here we report on the application of three reverse genetics mutagenesis tools: *M. truncatula* Tnt1

77   retrotransposon mutant collection (Tadege et al., 2008; Pislariu et al., 2012), hairpin RNA-interference

78   knock-down constructs (Wesley et al., 2001), and CRISPR/Cas9 site-specific nuclease (SSN) (Baltes et al.,

79   2014) to empirically evaluate the functional importance of ten genes that a previous sequence-based

80   GWA study identified as candidates for naturally occurring phenotypic variation in the legume-rhizobia

81   symbiosis (Stanton-Geddes et al., 2013). We used 17 whole-plant, stable mutants (six Tnt1, three hairpin,

82   and eight CRIPSR mutants) in well replicated phenotypic assays to evaluate the function of each of the

83   ten GWA candidates. The functional importance of three (*PHO2-like, PNO1- like and PEN3- like*) was

84   validated by two independent mutations, confirming the importance of genes found in three of the six

85   clusters investigated. These results not only identify genes not previously identified as being involved in

3

86   legume-rhizobia symbiosis, they also illustrate the power of combining GWA with newly-developed

87   gene-disruption technologies to identify genes that contribute to naturally occurring variation in

88   quantitative traits.

89

90

91

4

92   **RESULTS**

93

94   **Association mapping SNF-associate candidate genes in *Medicago***

95   To generate a list of candidates underlying variation in nodulation, we previously carried out GWA

96   analysis involving over 6 million SNPs on a panel of 226 *M. truncatula* accessions (Stanton-Geddes et al.,

97   2013). In brief, nodulation data were collected on eight replicates of each accession and GWA was

98   conducted using the GLMM implemented in TASSEL (Bradbury et al., 2007). From this GWA we selected

99   the 100 SNPs with the strongest association to variation in the number of nodules per plants, producing

100   an initial list of nodulation candidates. This list then was filtered based on several criteria: 1) Statistical

101   support and ranking for an association from the GWA, 2) Candidate being in linkage-disequilibrium (LD)

102   with other SNPs with strong statistical support (*i.e.*, located in a peak), 3) Location within or proximate

103   to annotated coding regions, and 4) Expression in root and or nodule tissue. GWA was performed twice

104   over the course of the research as a new assembly of the *M. truncatula* genome (Mt4.0) was released

105   mid-experiment (Tang et al., 2014), replacing the earlier assembly (Mt3.5) (Young et al., 2011) used in
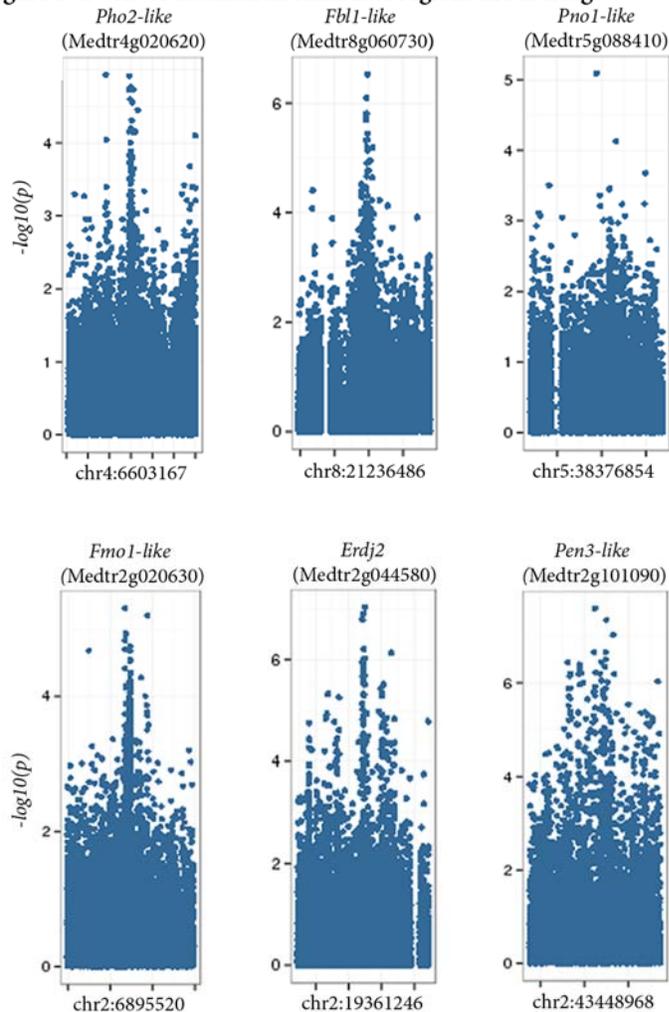
106   the original analysis.

107   Based on these criteria, we selected ten candidates (noting that we did not require all candidates to

108   meet all of the filtering criteria) to target for mutagenesis and phenotypic validation (Table 1). Six of the

109   candidates were physically proximate to other candidates (two within 15 kb of each other and four

110   within 80 kb of one another). These candidates were chosen to evaluate the potential to identify the

111   causative gene when clusters of statistically associated SNPs identified by GWA spanned multiple genes

112   (Fig. 1).

113

114   **Generation of whole plant mutants**

115   To empirically evaluate the functional importance of GWA-identified candidate genes underlying

116   naturally occurring variation in nodulation, we generated a suite of whole-plant mutants using three

117   mutagenesis platforms: Tnt1 retrotransposons, RNA hairpin knockdown, and CRISPR/Cas9 (SSNs) (Fig.

118   2a-c). We identified Tnt1 insertions in seven candidates by either querying the Noble Foundation Tnt1

119   database (Tadege et al., 2008) or through PCR screening of pools of Tnt1 mutant lines (Table S1). For

120   each of the seven putative Tnt1 mutants, we used a PCR assay with gene and insertion-specific primers

121   to identify lines that were either homozygous for the Tnt1 insertion or wild-type at the respective

122   candidate locus; hereafter referred to as *pho2-like$_{Tnt}$*, *fbl1-like$_{Tnt}$*, *pno1-like$_{Tnt}$*, *fmo1-like$_{Tnt}$*, *rfp1-like$_{Tnt}$*,

123   *hlz1-like$_{Tnt}$* and *pen3-like$_{Tnt}$* (Fig. 3a-c, Fig. S1, Fig. S9). We then used homozygous insertion and WT lines

5

Figure 1 GWAS of nodulation candidate regions in Medicago

Pho2-like
(Medtr4g020620)

Fbl1-like
(Medtr8g060730)

Pno1-like
(Medtr5g088410)

Fmo1-like
(Medtr2g020630)

Erdj2
(Medtr2g044580)

Pen3-like
(Medtr2g101090)

identified in this screen as parent plants to generate self-pollinated seeds for use in phenotype assays described below. Preliminary analyses revealed that the $fbl1_{Tnt}$ line as well as the WT line derived from the same grandparent plant were also segregating for a super-nodulating phenotype (> 100 nodules on root systems < 5 cm long), and therefore these were excluded from further analyses.

We also attempted to generate hairpin knock-downs for all ten candidates and successfully recovered multiple independently transformed whole plant mutant lines for four: *PHO2-like*, *FBL-like*, *PNO1-like*, and *ERDJ2*. Using TAIL-PCR we were able to determine the genomic location of hairpin transgene and identify homozygous hairpin lines for three of these genes, hereafter referred to as *fbl-like$_{HP}$*, *pno1-like$_{HP}$*, and *erdj2$_{HP}$* (Fig. 3b and Fig. S2a-c). These lines were grown to produce self-pollinated seed that was used for phenotype assays.
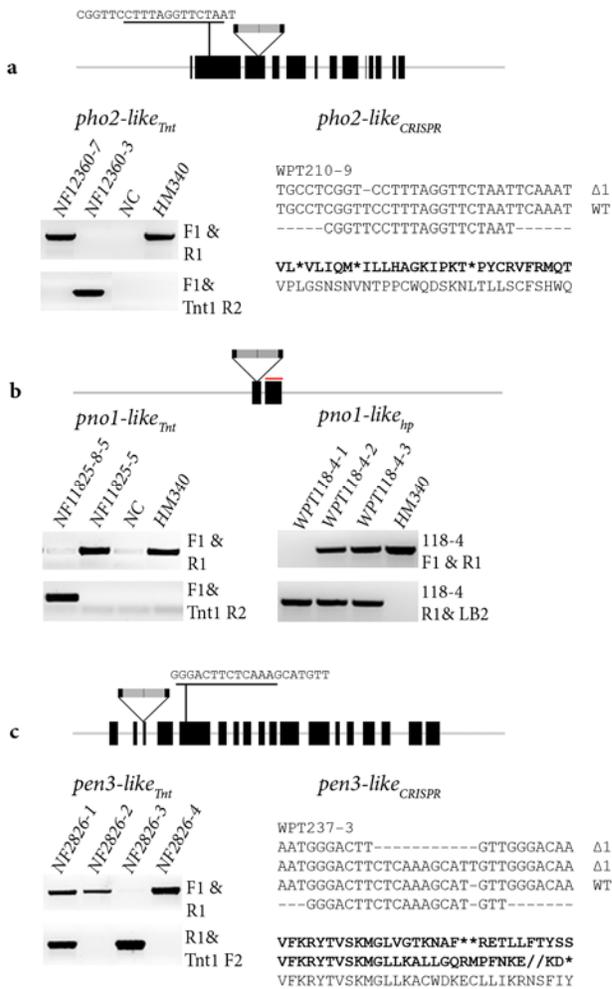
Because hairpin technologies are expected to reduce but not eliminate expression of target genes, we also targeted all ten candidates for whole-plant knock-outs using CRISPR/Cas9 and successfully generated whole-plant knock-out lines for seven candidate genes: *PHO2-like*, *FMO1-like*, *ERDJ2*, *ACRE1*,

6

Figure 2 Mutagenesis platforms

a *Tnt1 retrotransposon*

b *Hairpin knock-down*

c *CRISPR/Cas9 reagent*
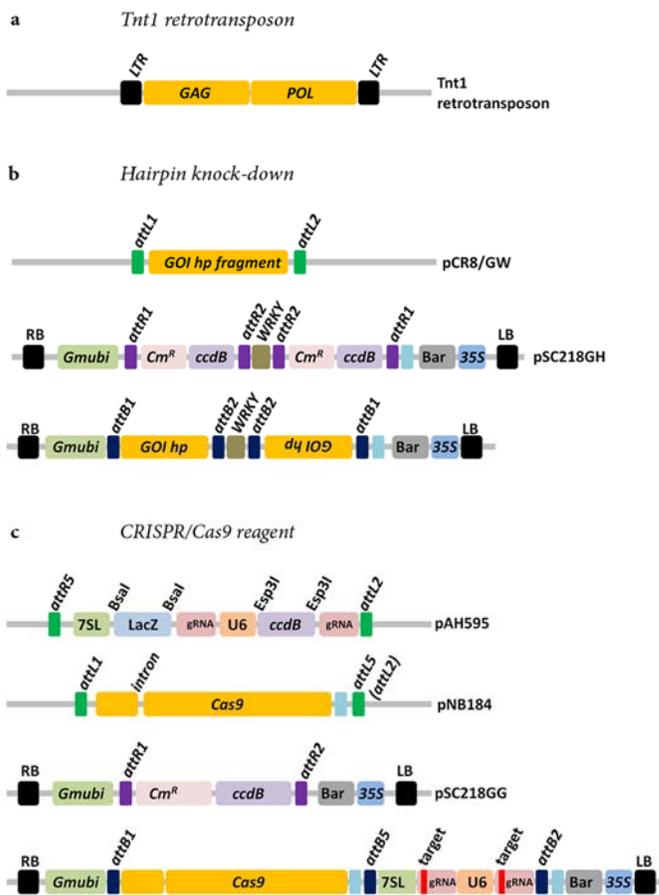
HLZ1-like, *MEL1* and *PEN3-like* (Fig. 3a-c and Fig. S3-S7). We recovered multiple T_0 homozygous mutant plants with mutation efficiencies ranging from 50-70% for many candidates genes including *PHO2-like, FMO1-like*, *ERDJ2*, and *PEN3-like* candidates, whereas germ-line mutations in *ACRE1*, *HLZ1-like*, *MEL1* mutant plants had to be confirmed in later generations (Fig. S3-S7). The CRISPR/Cas9 reagent was useful for mutating smaller sized genes (<500 bp) such as *Acre1* since the mutagenesis of these genes are typically more challenging using random mutagenesis strategies. Indeed, we could not identify a Tnt1 insertion in this gene by querying the Noble database and were also unsuccessful using the Tnt1 PCR-reverse-screen (Fig. S7a). By contrast, using the CRISPR system, we generated several *Acre1* candidate mutants and could generate mutations at the *ACRE2* paralog located 16-kbp upstream of *ACRE1* (Fig. S7b-c). For the *ERDJ2* candidate we recovered two T_0 homozygous mutant plants, one with a bi-allelic 3-bp and 85-bp frame-shift deletion and a second plant with two 6-bp mutant alleles (Fig. S4) and tested both mutants since we suspected the plant might be homozygous lethal. We hereafter referred to the

7

Figure 3 Screening of candidate mutant lines.

a

CGGTTCCTTTAGGTTCTAAT

pho2-like$_{Tnt}$

NF12360-7 NF12360-3 NC HM340

F1 & R1

F1& Tnt1 R2

pho2-like$_{CRISPR}$

```
WPT210-9
TGCCTCGGT-CCTTTAGGTTCTAATTCAAAT  Δ1
TGCCTCGGTTCCTTTAGGTTCTAATTCAAAT  WT
-----CGGTTCCTTTAGGTTCTAAT------

VL*VLIQM*ILLHAGKIPKT*PYCRVFRMQT
VPLGSNSNVNTPPCWQDSKNLTLLSCFSHWQ
```

b

pno1-like$_{Tnt}$

NF11825-8-5 NF11825-5 NC HM340

F1 & R1

F1& Tnt1 R2

pno1-like$_{hp}$

WPT118-4-1 WPT118-4-2 WPT118-4-3 HM340

118-4 F1 & R1

118-4 R1& LB2

c

GGGACTTCTCAAAGCATGTT

pen3-like$_{Tnt}$

NF2826-1 NF2826-2 NF2826-3 NF2826-4

F1 & R1

R1& Tnt1 F2

pen3-like$_{CRISPR}$

```
WPT237-3
AATGGGACTT----------GTTGGGACAA  Δ11
AATGGGACTTCTCAAAGCATTGTTGGGACAA  Δ1
AATGGGACTTCTCAAAGCAT-GTTGGGACAA  WT
---GGGACTTCTCAAAGCAT-GTT-------

VFKRYTVSKMGLVGTKNAF**RETLLFTYSS
VFKRYTVSKMGLLKALLGQRMPFNKE//KD*
VFKRYTVSKMGLLKACWDKECLLIKRNSFIY
```

149 CRISPR mutant lines as *pho2-like*$_{CRISPR}$, *fmo1-like*$_{CRISPR}$, *erdj2*$_{CRISPR-3/85}$, *erdj2*$_{CRISPR-6}$, *acre1-like*$_{CRISPR}$, *hlz1-*

150 *like*$_{CRISPR}$, *mel1*$_{CRISPR}$ and *pen3-like*$_{CRISPR}$. We were unable to confirm homozygous mutant plants for the

151 remaining three candidates (*FBL1-like*, *PNO1-like* and *RFP1-like*). The apparent poor mutation rate of

152 these three targets might be due to errors in the sequence used to construct the CRISPR reagent.

153 However, we grew all of the stable transformants to produce self-pollinated seeds that were then used

154 for phenotype assays.

155

156 **Mutation and knockdown of gene candidates affect nodulation**

157 We assayed nodule production in 17 mutant and paired control lines in a series of randomized and

158 well-replicated phenotype experiments. The assays were performed with an average of 22 mutant and

159 22 WT plants including six candidates tested with two independent mutation events to evaluate

160 whether results were robust to the specific mutation and genomic background.

8

161   Phenotype assays revealed that lines carrying mutations in three of the candidates, *PHO2-like*

162   (4g020620), *PNO1-like* (5g088410), and *PEN3-like* (2g101090), produced significantly fewer nodules than

163   control plants (P < 0.03 for each mutant by wild-type line comparison; Fig. 4a-c and Table S2). In each of

164   these cases, the phenotypic effects were validated by two independent mutations (Fig. 3). The *PHO2-*

165   *lik*e mutants were generated by the insertion of a Tnt1 element (*pho2-like$_{Tnt}$*) in one plant and a

166   CRISPR/Cas9 generated mutant harboring a homozygous 1-bp frame-shift mutation (*pho2-like$_{CRISPR}$*) in

167   the other. *PNO1-like* mutant plants were generated by insertion of a Tnt1 element (*pno1-like$_{Tnt}$*) and a

168   plant homozygous for a hairpin transgene targeting the *PNO1-like* transcript (*pno1-like$_{HP}$*). Similarly, two

169   *PEN3-like* mutants were identified by Tnt1 insertion (*pen3-like$_{Tnt}$*) and a CRISPR/Cas9 induced 11-bp and

170   1-bp bi-allelic frame-shift mutation in each allele (*pen3-like$_{CRISPR}$*) (Fig. 3a-c).

171   Surprisingly, two Tnt1 insertion lines (*fmo1-like$_{Tnt}$* and *hlz1-like$_{Tnt}$*) produced significantly more

172   nodules than control lines (Table S2). However, second mutations in these candidates, both generated

173   using CRISPR/Cas9, exhibited results inconsistent with the Tnt1 mutants ($P_{mut\_wt \times assay}$ < 0.05). Indeed, the

174   number of nodules formed by lines carrying CRISPR mutations in these genes did not differ from

175   controls. Potentially, the greater nodule number in the Tnt1 lines may have been due to Tnt1 insertions

176   in non-target genes (two of the control Tnt1 plants when assaying the *hlz1-like$_{Tnt}$* had no nodules and

177   five others had ≤ 10 nodules – many fewer than expected). Consequently, we decided to focus on the

178   three candidates with mutants showing reproducibly reduced nodule numbers compared than controls

179   (*PHO2-like*, *PNO1-like*, and *PEN3-like*) for further analysis.

180

181   **Nitrogen content and nodule morphology of validated candidate lines**

182   Although plants with mutations in the three validated candidate genes (*PHO2-like*, *PNO1-like*,

183   *PEN3-like*) produced significantly fewer nodules, N concentration and nodule morphology were not

184   affected. Foliar nitrogen concentrations did not differ significantly between any of the mutants and their

185   control (t-tests, all $p_{df=4}$ > 0.1, Supplemental Table S2). Moreover, longitudinal sections of nodules from

186   all validated mutant lines indicated they were structurally sound, with distinct meristematic, infection,

187   and pink nitrogen fixation zones (Supplemental Figs. S10, S11). Both *pho2-like$_{tnt1}$* mutants and their

188   corresponding WT controls had lighter pink nodules overall, however *pho2-like$_{CRISPR}$* nodules exhibited

189   similar color intensity compared with the HM340 control (Fig. S11). This suggests that differences in the

190   pink color of *Pho2-like$_{tnt1}$* is probably due to the Tnt1 background rather than disruption of the *PHO2-like*

191   gene itself.

192

9

Figure 4 Distribution of nodule number produced by mutant and wild
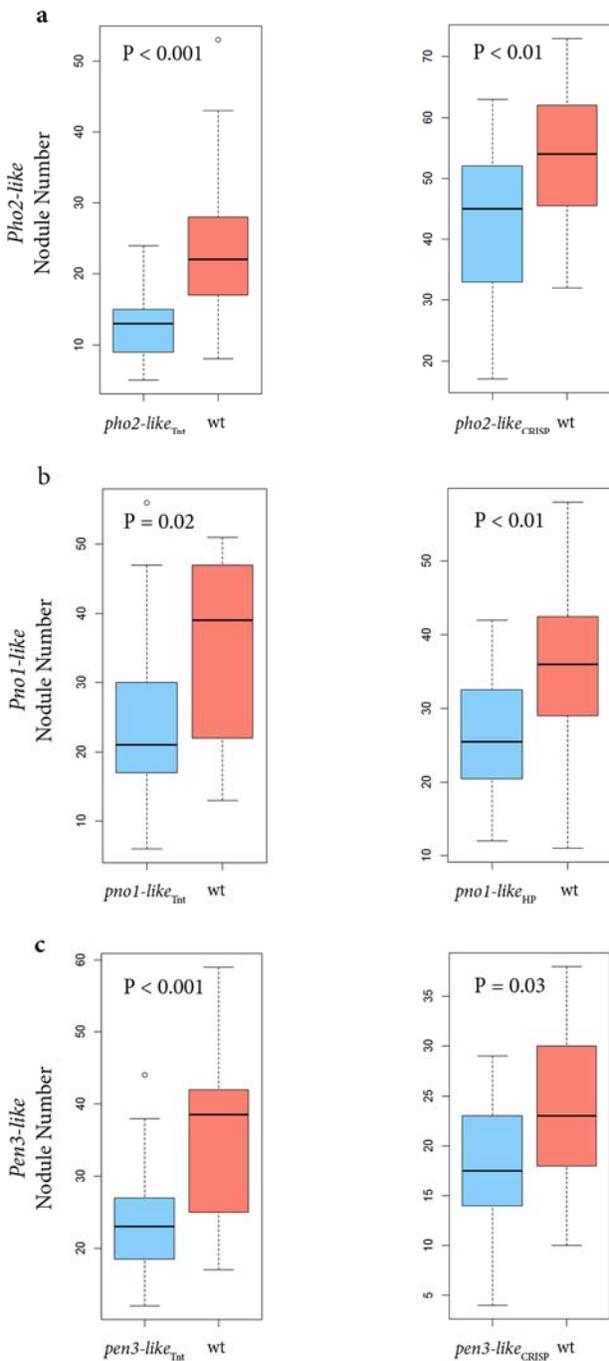
Effects of forward genetic mutants

193

194   To better understand the quantitative nature of nodulation mutants, we compared effects of the

195   validated GWA mutants to nodulation mutants in genes originally discovered through forward genetics.

196   Considering only "confirmed" candidates from our GWA study (*PHO2-like*, *PNO1-like*, *PEN3-like*), GWA

197   mutants produced ~ 60% of the number of nodules on wild-type plants. These results were then

10

198   compared to phenotype assays on two well-known and previously characterized nodulation mutant

199   lines: the calcium and calmodulin-dependent kinase *dmi3* (Catoira et al., 2000) and *ipd3-2*, which

200   encodes for a protein that interacts with DMI3 (Messinese et al., 2007). Under exactly the same

201   experimental conditions used to test the GWA mutant lines, these forward genetics mutants exhibited

202   drastic reductions in nodule number – an average of just 0.5 nodules on *dmi3* lines and 1.5 nodules on

203   *ipd3* lines compared with 39 on WT plants (P < 0.0005, Fig. S8).

204

205

206

11

DISCUSSION

208   Genome wide association analyses provide an opportunity for identifying functionally important

209   genes that contribute to naturally occurring variation in quantitative traits, genes that are unlikely to be

210   detected by forward genetic screens. However, the approach is challenged by several statistical issues

211   including an expected high number of statistical false positives due to the large number of statistical

212   tests and the difficulty of fully eliminating confounding effects of relatedness among assayed individuals.

213   This means that GWA is best viewed as a statistical approach for identifying genomic regions that are

214   likely to contribute to variation. Moving beyond such a candidate status requires empirical validation of

215   gene function (Ioannidis et al., 2009). In this work, we applied a suite of mutagenesis platforms,

216   retrotransposon insertions, hairpin knock-down RNAi constructs, and CRISPR/Cas9, to disrupt the

217   function of ten genes that GWA had identified as candidates in contributing to variation in the legume-

218   rhizobia symbiosis through nodulation (Stanton-Geddes et al., 2013). Our evaluation experiments

219   revealed that mutations in three of the ten candidate lines produced significantly fewer nodules than

220   wild-type plants, thereby identifying new genes contributing to quantitative variation in nodule

221   production.

222   Three out of ten candidate genes were empirically validated in this study. However, there was more

223   than one candidate gene for some genomic intervals. Therefore, the validation rate is better

224   represented as three validated genes among the six intervals evaluated. These findings demonstrate

225   that GWA coupled with well-replicated validation experiments is an effective means to identify genes

226   contributing to quantitative variation. The high rate of success in validating the functional importance of

227   GWA candidates is likely due to at least two reasons. First, in creating an initial list of candidates for

228   functional evaluation, we did not limit our efforts to only those variants with the strongest statistical

229   support from the GWA. Rather, we considered the 100 SNPs with the strongest statistical associations

230   with phenotypic variation as potential candidates and then applied genetically informed criteria for

231   identifying which candidates to pursue for validation. These criteria included SNPs in or near annotated

232   genes, genes expressed in roots or nodules, and SNPs that formed clusters of statistical associations,

233   (peaks in the Manhattan plots) (Fig. 1).

234   Despite the criterion that chosen SNPs either were in or near a coding region, only four of the GWA

235   variants that we pursued were actually in annotated coding regions, with the remainder anywhere from

236   168 to 5819 bp from annotated CDS. Our data do not allow us to determine whether the SNPs near, but

237   not in, coding regions cause functionally important variation in gene expression as opposed to linkage-

238   disequilibrium (LD) with un-assayed SNPs in coding regions. Nevertheless, non-coding SNPs are often

12

239 associated with phenotypic variation (Hindorff et al., 2009) through effects on gene expression (Cookson

240 et al., 2009; Cubillos et al., 2012). We also prioritized candidates that showed expression in root or

241 nodule tissue, although such a criterion might have biased against lowly expressed genes (like many

242 transcription factors) or gene products expressed elsewhere in the plant affecting nodulation (Krusell et

243 al., 2002). The third criterion we applied, that candidates be physically proximate to other SNPs showing

244 strong associations, is likely to favor alleles that are maintained in contemporary populations through

245 balancing selection where the optimal trait value varies among populations or that have recently

246 increased in frequency (Barton and Turelli, 1989; Yeaman and Whitlock, 2011).

247 Also central to our evaluation experiments was the use of well-replicated experiments when

248 evaluating phenotypic effects. Each of the phenotypic assays we conducted involved an average of 22

249 mutant and 22 WT (minimum of 7 mutant and 6 wild-type) individuals. This was important because the

250 distributions of mutant and WT phenotypes often showed considerable overlap (Fig. 4a-c). The

251 importance of replication also helps to explain why the genes we identified had not been detected in

252 earlier forward-genetic screens conducted on nodulation in *M. truncatula* (Catoira et al., 2000; Oldroyd

253 and Long, 2003; Schnabel et al., 2005; Pislariu et al., 2012; Domonkos et al., 2013). If the mutations we

254 evaluated had been tested in only a single individual, the mutant phenotype would likely have fallen into

255 the range of phenotypes exhibited by WT plants generally and thus would not have been picked up in a

256 standard genetic screen. The phenotypic effects of genes identified through forward genetic screens

257 relative to those we validated here is highlighted by the comparison of *dmi3* and *ipd3* to the three GWA-

258 selected candidates: *dmi3* and *ipd3* plants produced an average of approximately 2% of the number of

259 nodules produced on WT plants whereas the validated genes first identified as candidates through GWA

260 produced roughly 60% of the number of nodules compared with WT plants.

261

262 **Genetics of nodulation**

263 Although we identified candidates without prior knowledge of their function, the molecular

264 functions of homologs for the validated candidates are known and all are interesting in the context of

265 nodulation. One of the validated candidates, *PHO-like* (Medtr4g020620), suggests a potentially

266 important role for phosphorous in quantitative variation in nodulation. *PHO2-like* is annotated as

267 encoding an E2 ubiquitin conjugating enzyme and its *Arabidopsis thaliana* ortholog (35% AA identity, E

268 value = 4e-104) is involved in phosphorous accumulation (Park et al., 2014). Not only can phosphorous

269 availability affect nodulation and N_2 fixation (Graham and Rosas, 1979; Jakobsen, 1985; Graham, 1992,

270 Sulleman 2013) but in *A. thaliana*, *AtPHO2* ortholog interacts directly with the E3 product of Nitrogen

13

271   Limitation Adaption (*Nla*), which mediates plant responses to N limitation (Park et al., 2014). Moreover,

272   E2 ubiquitin conjugate enzymes are presumed to interact with multiple E3 partners that could lead to

273   the proteolytic degradation of a larger range of uncharacterized substrates (Smalle and Vierstra, 2004).

274   *Medicago PHO2-like* is expressed at modest levels throughout nodule development (and also in

275   uninoculated roots), but reaches a distinct peak in expression at 20 dpi (Fig. S12). This is a timepoint

276   when nodules are fully differentiated, actively fixing nitrogen, and still prior to the initiation of

277   senescence.

278   A second interesting validated gene is the annotated ABC transporter (*PEN3-like*) (Medtr2g101090).

279   ABC transporters are involved in a wide range of plant activities, including pathogen metabolite

280   detoxification, non-host pathogen resistance, stomatal function, and Ca^{2+} sensing associated plant

281   immunity (Rea, 2007; Campe et al., 2016). The *A. thaliana* gene with greatest similarity to

282   Medtr2g101090 is *PEN3* (66% identical AA sequence across 97% of the gene length. E-value = 0), which

283   has been shown to be an essential component of salicylic acid-related defense against biotrophic fungi

284   (Stein et al., 2006; Johansson et al., 2014). The formation of nodules requires direct interaction with

285   bacteria and there is growing evidence that defense responses can negatively affect nodule formation

286   (Ramu et al., 2002; Lopez-Gomez et al., 2012; Larrainzar et al., 2015). Interestingly, ABC transporters

287   have been shown to be significantly and highly up-regulated in several nodulation mutants relative to

288   wild-type controls (Lang and Long, 2015). *PEN3-like* is strongly expressed in *Medicago* nodules

289   throughout development, though even more highly expressed in roots, with a slight peak in nodule

290   expression at 14 dpi (Fig. S12).

291   The final validated candidate is annotated as encoding an RNA-binding *PNO1-like* protein

292   (Medtr5g088410). How this protein might affect nodulation is not clear, although recent work has

293   identified roles for members of this gene family in the regulation of miRNAs (Karlsson et al., 2015),

294   suggesting that Medtr5g088410 could affect the expression of genes involved in nodulation. It is

295   expressed at a comparatively low level in both nodules and roots with no distinct peak in time of

296   expression (Fig. S12).

297

298

299   **Mutation platforms for GWA validation**

300   Efficient means to validate the functional importance of GWA candidate genes are necessary for

301   GWAS to be effective in discovering genes of subtle effects, fulfilling the promise of linking molecular

302   genetics with quantitative trait variation. Here we applied multiple genomic technologies

14

303   (retrotransposon mutagenesis, hairpins, and CRISPR/Cas9) to make this link. Each of these technologies

304   has advantages and disadvantages when being applied as a reverse genetics tool. The *M. truncatula*

305   Tnt1 collection has the advantage of ease: the Noble Foundation in Ardmore, OK has over 21,000

306   mutant lines that have largely saturated the genome with random Tnt1 insertion events and the

307   collection is easily searchable online. Although easy to use for validation experiments, there is the

308   problem of background mutations (*e.g.,* Fig. S9). On average, there are 25 insertions in each Tnt1 lines

309   and as many as 97 independent Tnt1 loci have been reported (Veerappan et al., 2016). These

310   background mutations can make phenotyping data potentially unreliable, complicating their use as the

311   sole validation tool in reverse genetics phenotyping experiments. In our experiments, one Tnt1 line

312   expressed an (unexpected) super-nodulation phenotype, while two Tnt1 lines produced more nodules

313   than control plants, though neither of these phenotypes could be validated with a second (non-Tnt1)

314   mutation.

315   Both hairpin and CRISPR require more effort to create, involving construction of vectors, infecting

316   plants with *Agrobacterium*, and regeneration of whole plants from callus. Despite these challenges, we

317   had a high rate of success in creating stable whole-plant transformants using both hairpin and

318   CRISPR/Cas9 at high efficiency and frequency. For example, CRISPR/Cas9 targeting the *PHO2-like* and

319   *PEN3-like* genes induced homozygous mutations in multiple independent T_0 plants (Fig S3- S7).

320   Hairpin technologies seem promising in two situations: when genes of interest are members of

321   multi-gene families where gene redundancy might mask phenotype effects and for genes that are

322   gametophytic or homozygous lethal. This is illustrated by the *ERDJ2* candidate in our mutant screening.

323   We identified a CRISPR/Cas9 *ERDJ2* mutant with an in-frame 3-bp and a frame-shift 85-bp mutant alleles

324   and confirmed that the gene is homozygous lethal by segregation analysis. PCR analysis of

325   approximately 30 *erdj2$_{CRISPR\_3/85}$* mutants failed to identify plants with both frame-shift 85-bp mutant

326   alleles, suggesting that the combination of frame shift mutations results in a homozygous lethal

327   phenotype (Fig. S4). Nevertheless, we successfully created a hairpin mutant that decreased transcript

328   expression without the lethality of a knock-out to use in candidate validation. For some genes, however,

329   "knocking down" rather than "knocking out" expression could also limit the phenotypic effects of the

330   mutations.

331   CRIPSR technologies have advanced rapidly in recent years and hold promise for altering gene

332   sequence and expression in many systems including plants (Baltes and Voytas, 2015; Luo et al., 2016).

333   Although producing stable germ-line whole-plant mutants has proven challenging in some species,

334   including *A. thaliana* (Fauser et al., 2014; Feng et al., 2014), we were able to produce stable mutant lines

15

335 with high efficiency. The mechanism behind this success rate is not clear, although we suspect that the

336 transformation method might be a factor. *Medicago* transformation generates callus tissue that

337 undergoes strong herbicide selection in contrast to floral dip transformation that requires infection of

338 individual embryos. Moreover, we were often able to remove the CRISPR transgene from the mutant

339 lines by genetic segregation to obtain non-transgenic mutant plants that can be used for future

340 complementation studies. Given the rapid development of CRISPR multi-plex platforms, it should soon

341 be feasible to mutate and test large numbers of GWA identified candidates. Doing so would allow

342 researchers to move beyond validating small numbers of candidates and allow robust empirical

343 evaluation of the genes that control variation underlying complex quantitative traits.

344

345 **MATERIALS AND METHODS**

346

347 **Insertional mutant screening and genotyping**

348 To identify mutants in the 10 candidates selected for validation, we first searched for Tnt1

349 insertional mutants using the Noble Foundation's *M. truncatula* Mutant Database (http://medicago-

350 mutant.noble.org/mutant/blast/blast.php) (Tadege et al., 2008; Pislariu et al., 2012). Searches of this

351 database, which is comprised of more than 21,000 mutants, identified insertions in five of seven

352 candidates with the remaining two candidates identified by a PCR reverse-screen performed at the

353 Noble Foundation (Table S1). Seeds for Tnt1 mutant lines were obtained from the *M. truncatula* Tnt1

354 collection, planted, and genotyped for homozygous and wild-type (null) insertion alleles at the locus of

355 interest. Mutant plants for *Erdj2*, *Acre1* and *Mel1* candidates could not be identified either from the

356 Tnt1 database or from the PCR-reverse screen and we therefore relied upon the CRISPR/Cas9 platform

357 to generate these mutants.

358

359 **Hairpin and CRISPR/Cas9 transgenes and whole plant transformation**

360 We attempted to create hairpin constructs to reduce gene expression in all 10 candidates and

361 successfully identified homozygous hairpin transgenic plant lines for three: *FBL1-like*, *PNO1-like*, and

362 *ERDJ2*. To create hairpins, targeted coding sequences were amplified by PCR using primer sequences

363 (Table S3) from cDNA derived from *M. truncatula* accession R108. These amplicons were cloned into the

364 pCR8/GW/TOPO entry vector (Life Technologies, CA) and incorporated into the hairpin destination

365 vectors pSC218GH (see below) by a Gateway™ LR clonase reaction.

16

366   Finally, we generated CRISPR/Cas9 SSN to introduce frame-shift mutations in all 10 candidates and

367   recovered homozygous mutants for seven. Target sequences were identified by BLAST searches of the

368   *Medicago* R108 (HM340) genome assembly (www.medicagohapmap.org/downloads/r108) using the Mt

369   4.0 reference sequence as a query. Resulting sequences were then used to query the sgRNA designer v.1

370   for selection of target guide RNAs (www.broadinstitute.org/rnai/public/analysis-tools/sgrna-design-v1)

371   (Doench et al., 2014). The targets were created by a primer annealing assay and cloned into the *Esp3*I

372   and *Bsa*I sites of the U6/At7SL guide RNA entry vector (pAH595) (Table S3). The completed guide RNA

373   entry vector sequence was confirmed and combined with a second entry vector that harbored the

374   *Arabidopsis* optimized Cas9 cassette (pNJB184) by a multi-site Gateway LR clonase reaction into the

375   pSC218GG destination vector (see below) for *Agrobacterium* transformation (Li et al., 2013; Baltes et al.,

376   2014). A detailed protocol can be found in the Supplemental Methods.

377   Whole plant transformation of R108 plants, the same genetic background used in the *M. truncatula*

378   Tnt1 collection, with hpRNA and CRISPR/Cas9 constructs was carried out using a slightly modified

379   version of an established protocol (Cosson et al., 2006). In brief, transformation was carried out by

380   inoculating leaf tissue explants with *A. tumefaciens* strain EAH105 transformed with either a hairpin or

381   CRISPR SSN. The transformations were conducted using a modified version of the binary vector

382   backbone pNB96 (pSC218) (Curtin et al., 2011) with an introduced inverted-repeat cassette to facilitate

383   cloning of hairpin RNA fragments (pSC218GH) and a reading-frame cassette to incorporate both the

384   Cas9 and target guide RNA entry vectors (pSC218GG). The inverted-repeat and reading-frame cassettes

385   were derived from previously reported pTDT-DC-RNAi and pTDTO vectors (Valdes-Lopez et al., 2008)

386   and were driven by the constitutively expressed *Glycine max* Ubiquitin promoter (Hernandez-Garcia et

387   al., 2010).

388   After co-cultivating the leaf tissue with *Agrobacterium* for three days, explants were washed in an

389   antibiotic liquid media and transferred to a media for callus induction with bi-weekly transfers. After

390   approximately six weeks, callus tissue was transferred to a shoot induction media and incubated in 16:8

391   light:dark hour photoperiod. Developing shoots were transferred to a rooting media to encourage root

392   development before planting to soil. Both binary vectors pSC218GH and pSC218GG contain the 35S::BAR

393   cassette for phosphinothricin herbicide selection of transgenic plants. T_0 plants were rapidly screened

394   using a previously reported DNA extraction method and PCR-CAPS assay to identify target mutations

395   (Curtin et al., 2011).

396

397   **Nodulation assays**

17

398   To evaluate the effects of candidate gene mutations on nodulation we grew mutant and wild-type

399   plants in well-replicated (an average of 22 mutant and 22 wild type plants per assay, see Table S2 for

400   details) in completely-randomized experiments. Prior to planting, seeds were treated in concentrated

401   sulfuric acid for 5 min, washed with sterile dH_2O, and then kept in the dark on wet filter paper at 4°C for

402   7–10 days before planting into 650 ml conetainers with 4:1 parts autoclaved sand:perlite mixture. Five

403   days after planting, seedlings were inoculation with a 30mL suspension (OD600 ~0.015) of *S. meliloti*

404   strain Sm2011 carrying the *hemA*::LacZ reporter (Ardourel et al., 1994). Plants were grown at 22-25°C,

405   75 % humidity and 200-350 $\mu molm^{-2}s^{-1}$ 16h-8 h photoperiod, fertilized 15 and 21 days post inoculation

406   with Fähreus nutrient solution, and otherwise watered as needed. Thirty-five to 41 days after

407   inoculation, plants were harvested and nodule number was determined. Each mutant was compared

408   against a separate set of WT control plants. To reduce the effects of background insertions, controls for

409   the Tnt1 mutants were grown from seeds from a full-sib of the mutant plants. R108 seeds were used for

410   the control treatment for hairpin and CRISPR lines. For each assay experiment, we tested for statistically

411   significant differences between the phenotype of the mutant line and the phenotype of the wild-type

412   control line using a t-test using R (R Development Core Team, 2013). For the six candidates (*PHO2-like*,

413   *PNO1-like*, *FMO1-like*, *ERDJ2*, *HLZ1-like* and *PEN3-like*) where we evaluated two independent mutation

414   lines, we also used ANOVA to test for between-line differences in nodulation. Similarly, for the two

415   mutant lines (*pho2$_{CRIPSR}$, mel1$_{CRISPR}$*) for which the phenotypic assays were repeated, we used ANOVA to

416   test for differences between mutant and wild-type lines between assays. All data are available at

417   datadryad.org (dx.doi.org xxxxxxxx).

418

419   **Nodule morphology and nitrogen content**

420   To complement phenotypic data collected during initial validation experiments, we also grew the

421   three mutants exhibiting validated nodulation phenotypes (*PHO2-like*, *PNO1-like*, and *PEN3-like*) to test

422   for differences in foliar N concentration and to examine nodule morphology. These plants were grown

423   under the same conditions as those for initial phenotype assays. At 14 dpi, three plants per treatment

424   were harvested in order to make visual observations of nodules. Plants were washed to remove

425   surrounding substrate and 10 cm of roots with nodules were isolated to obtain close up pictures of

426   nodules (Figure S10). One nodule (second or third from the top) was then harvested from each plant,

427   sliced in half longitudinally by hand, and then observed under a stereo microscope (Figure S11). At 28

428   dpi, four plants grown in parallel were harvested for N concentration assays, which were conducted by

429   the University of Minnesota Research Analytical Lab using the Dumais method (Matejovic, 1995).

18

430

431

432

433

434   **Table 1.** Genome Location, GWAS statistics, and Expression of Candidate Genes

435

Mt4.0 Designation	Candidate Gene	Rank	P-value	GWAS	Expression	Confirmed
Medtr2g020630	Flavin-containing Monooxygenase-like (FMO1-LIKE)	41	8.14E-06	Mt3.5	Root & nodule specific	
Medtr2g044570	Ring finger protein1-like (RFP1-like)	8	1.62E-07	Mt3.5	All tissues	
Medtr2g044580	Endoplasmic reticulum DNAJ protein (ERDJ2)	5	1.30E-07	Mt3.5	Nodule upregulated	
Medtr2g101040	Malic enzyme-like1 (MEL1)	15	2.22E-07	Mt4.0	All tissues	
Medtr2g101090	Penetration3-like (PEN3-like)	1	2.56E-08	Mt4.0	Root & nodule upregulated	YES
Medtr2g101120	AVR9/CF-9 rapidly elicited protein 1 (ACRE1)	23	3.55E-07	Mt4.0	All tissues	
Medtr2g101190	Homeodomain leucine zipper1-like (HLZ1-like)	72	9.65E-07	Mt4.0	All tissues	
Medtr4g020620	Ubiquitin conjugate24 like (PHO2-like)	12	5.58E-06	Mt3.5	Nodule upregulated	YES
Medtr5g088410	Partner of NOB1-like (PNO1-like)	36	7.08E-06	Mt3.5	Root & nodule specific	YES
Medtr8g060730	F-box like 1 (FBL1-like)	2	4.26E-08	Mt3.5	Below detection limit	

436

437

20

438

FIGURE LEGENDS

Figure 1. GWAS of nodulation candidate regions in *Medicago*. From left to right, Manhattan plots extending 300,000 bp either side of the candidate SNP for each of the six candidate gene regions.

Figure 2. Mutagenesis platforms. a. Tnt1 retrotransposon insertional mutagenesis in *Medicago* was developed in the R108 (HM340) accession. The original transformant harbored five Tnt1 copies. The Tnt1 element can transpose by a copy and paste mechanism during callus regeneration leading to progeny lines with random stable insertions. **b.** Schematic representations of the hairpin entry and destination vectors. Typically, a 300-500 bp amplicon from the candidate gene of interest is amplified from *Medicago* whole-plant cDNA template and cloned into the pCR8/GW entry vector. The entry vector is then used to clone the hairpin fragment into the pSC218GH binary vector, followed by *Agrobacterium* transformation. **c.** The construction of the CRISPR/Cas9 reagent requires a multi-site Gateway cloning reaction utilizing two entry vectors and a destination binary vector. The CRIPSR targets are cloned into pAH595, and along with the Cas9 entry vector (pNB184) are cloned into pSC218GG vector, followed by *Agrobacterium* transformation. A detail protocol of the CRISPR/Cas9 assembly is provided in the Supplemental Methods.

Figure 3. Screening and identification of candidate mutant alleles. a. Two independent *PHO2-like* mutant alleles, *pho2-like$_{Tnt}$* and *pho2-like$_{CRISPR}$*. Seeds from the Tnt1 line NF12360 were screened by PCR assay to determine homozygous and null insertions at the *PHO2-like* locus, identifying null insertion NF12360-8 plant and homozygous mutant NF12360-7 (Supplemental Figure S9). A second mutant allele for *PHO2-like* was identified using plants transfromed with a CRISPR/Cas9 reagent that targeted the open-reading frame of *PHO2-like*. Several homozygous T$_0$ mutant plants were identified and the WPT210-9 plant was selected for downstream phenotype analyses. WPT210-9 had a 1-bp deletion in the coding region of both alleles, effectively disrupting the reading frame as indicated by the three stop codons depicted in the amino acid sequence. Heritable transmission of the 1-bp mutation was confirmed by screening T1 plants by a PCR-digestion assay and sequencing. **b**. Two independent *PNO1-like* mutant alleles, *pno1-like$_{Tnt}$* and *pno1-like$_{HP}$*.Tnt1 mutant alleles were identified for *PNO1-like* by screening seed from the NF11825 line. *Pno1-like* mutant and null insertion lines were identified, NF11825-8 and NF11825-5 respectively. Since an insufficient number of seed was recovered from the NF11825-8 plant for phenotype analysis, seed from the next generation (NF11825-8-5) was used as wild-type plant. For the second mutant allele, a hairpin line was identified. TAIL

21

473　PCR was used to identify the genomic location of the transgene and a PCR assay using both the
474　genome location and transgene specific primers were used to identify a plant homozygous for
475　the hairpin transgene (WPT118-4-1). **c,** Two independent *PEN3-like* mutant alleles, *pen3-like$_{Tnt}$*
476　and *pen3-like$_{CRISPR}$*. Seed from the NF2826 Tnt1 line were used to identify homozygous (NF2826-
477　4) and null (NF2826-2) insertion mutant plants using both *PEN3-like* and Tnt1 specific primers.
478　For the second mutant allele, we identified several CRISPR/Cas9 homozygous T$_0$ mutant plants
479　such as WPT237-3 which had a segreagting a bi-allelic mutation consisting of a 11bp deletion
480　and a 1bp insertion. Screening of WPT237-3 T1 mutant plants confirmed heritable transmission
481　of both mutations.
482
483　**Figure 4. Nodule number produced by mutant and wild type plants**. Nodules were counted 32-
484　42 days post inoculation. Data are shown for two independent mutants for each of three
485　candidate genes. a, *PHO2-like*, b, *PNO1-like*, and c, *PEN3-like*. For each figure, the horizontal
486　black bar represents the median value, the box the middle quartiles, and the whiskers the range
487　of data, except for outliers shown as a single data point.
488
489
490
491
492
493
494

22

495
496
497
498
499
500
501
502 **Supplemental Data**
503
504 The following supplemental materials are available.
505
506 **Supplemental Figure S1.** The characterization of three Tnt1 mutant lines
507 **Supplemental Figure S2.** The characterization of two whole-plant hairpin lines
508 **Supplemental Figure S3.** The characterization of the Pho2-like CRISPR/Cas9 mutants
509 **Supplemental Figure S4.** The characterization of the Erdj2 CRISPR/Cas9 mutants
510 **Supplemental Figure S5**. The characterization of the Acre-1 CRISPR/Cas9 mutants
511 **Supplemental Figure S6.** The characterization of the Pen3-like CRISPR/Cas9 mutants
512 **Supplemental Figure S7**. The characterization of the Fmo1-like, Hlz-1 and Mel1-like CRISPR/Cas9
513 mutants
514 **Supplemental Figure S8**. Nodulation phenotype of dmi3 and ipd3-2
515 **Supplemental Figure S9.** The Tnt1 insertion background of the NF12360 Tnt1 mutant line
516 **Supplemental Figure S10.** WT and Pho2-like, Pen3-like, and Pno1-like mutant nodules at 14 dpi
517 **Supplemental Figure S11**. WT and Pho2-like, Pen3-like, and Pno1-like mutant dissected nodules at 14
518 dpi
519 **Supplemental Figure S12**. The expression analysis of validated genes, derived from the Medicago
520 truncatula Gene Expression Atlas ((http://mtgea.noble.org/v3/index.php)
521
522 **Supplemental Table S1**. List of Tnt1 mutant lines obtained from Noble Foundation Tnt1 mutant
523 database
524 **Supplemental Table S2**. Statistical tests comparing phenotype between mutant and wild-type control
525 plants
526 **Supplemental Table S3**. Primer sequences for PCR assays and vector construction (SEPARATE EXCEL
527 FILE)
528
529 **Supplemental Methods 1.** CRISPR reagent design and construction
530
531
532
533 **ACKNOWLEDGMENTS**
534

23

539

540

541

542

24

Parsed Citations

Ardourel M, Demont N, Debellé F, Maillet F, de Billy F, Promé JC, Dénarié J, Truchet G (1994) Rhizobium meliloti lipooligosaccharide nodulation factors: different structural requirements for bacterial entry into target root hair cells and induction of plant symbiotic developmental responses. Plant Cell 6: 1357-1374
Pubmed: Author and Title
CrossRef: Author and Title
Google Scholar: Author Only Title Only Author and Title

Baltes NJ, Gil-Humanes J, Cermak T, Atkins P a, Voytas DF (2014) DNA replicons for plant genome engineering. Plant Cell 26: 151-63
Pubmed: Author and Title
CrossRef: Author and Title
Google Scholar: Author Only Title Only Author and Title

Baltes NJ, Voytas DF (2015) Enabling plant synthetic biology through genome engineering. Trends Biotechnol 33: 120-131
Pubmed: Author and Title
CrossRef: Author and Title
Google Scholar: Author Only Title Only Author and Title

Barton NH, Turelli M (1989) Evolutionary Quantitative Genetics: How Little Do We Know? Annu Rev Genet 23: 337-370
Pubmed: Author and Title
CrossRef: Author and Title
Google Scholar: Author Only Title Only Author and Title

Bradbury PJ, Zhang Z, Kroon DE, Casstevens TM, Ramdoss Y, Buckler ES (2007) TASSEL: Software for association mapping of complex traits in diverse samples. Bioinformatics 23: 2633-2635
Pubmed: Author and Title
CrossRef: Author and Title
Google Scholar: Author Only Title Only Author and Title

Campe R, Langenbach C, Leissing F, Popescu G V., Popescu SC, Goellner K, Beckers GJM, Conrath U (2016) ABC transporter PEN3/PDR8/ABCG36 interacts with calmodulin that, like PEN3, is required for Arabidopsis nonhost resistance. New Phytol 209: 294-306
Pubmed: Author and Title
CrossRef: Author and Title
Google Scholar: Author Only Title Only Author and Title

Catoira R, Galera C, de Billy F, Penmetsa R V, Journet EP, Maillet F, Rosenberg C, Cook D, Gough C, Dénarié J (2000) Four genes of Medicago truncatula controlling components of a nod factor transduction pathway. Plant Cell 12: 1647-66
Pubmed: Author and Title
CrossRef: Author and Title
Google Scholar: Author Only Title Only Author and Title

Cookson W, Liang L, Abecasis G, Moffatt M, Lathrop M (2009) Mapping complex disease traits with global gene expression. Nat Rev Genet 10: 184-194
Pubmed: Author and Title
CrossRef: Author and Title
Google Scholar: Author Only Title Only Author and Title

Cosson V, Durand P, D'Erfurth I (2006) Medicago truncatula transformation using leaf explants. Methods Mol Biol. 343: 115-127
Pubmed: Author and Title
CrossRef: Author and Title
Google Scholar: Author Only Title Only Author and Title

Cubillos F, Coustham V, Loudet O (2012) Lessons from eQTL mapping studies: non-coding regions and their role behind natural phenotypic variation in plants. Curr Opin Plant Biol 15: 192-198
Pubmed: Author and Title
CrossRef: Author and Title
Google Scholar: Author Only Title Only Author and Title

Curtin SJ, Zhang F, Sander JD, Haun WJ, Starker C, Baltes NJ, Reyon D, Dahlborg EJ, Goodwin MJ, Coffman AP, et al (2011) Targeted mutagenesis of duplicated genes in soybean with zinc-finger nucleases. Plant Physiol 156: 466-73
Pubmed: Author and Title
CrossRef: Author and Title
Google Scholar: Author Only Title Only Author and Title

Doench JG, Hartenian E, Graham DB, Tothova Z, Hegde M, Smith I, Sullender M, Ebert BL, Xavier RJ, Root DE (2014) Rational design of highly active sgRNAs for CRISPR-Cas9-mediated gene inactivation. Nat Biotechnol 32: 1262-7
Pubmed: Author and Title
CrossRef: Author and Title
Google Scholar: Author Only Title Only Author and Title

Domonkos A, Horvath B, Marsh JF, Halasz G, Ayaydin F, Oldroyd GED, Kalo P (2013) The identification of novel loci required for appropriate nodule development in Medicago truncatula. BMC Plant Biol 13: 157
Pubmed: Author and Title
CrossRef: Author and Title
Google Scholar: Author Only Title Only Author and Title

Fauser F, Schiml S, Puchta H (2014) Both CRISPR/Cas-based nucleases and nickases can be used efficiently for genome

engineering in Arabidopsis thaliana. Plant J 79: 348-359

Pubmed: Author and Title
CrossRef: Author and Title
Google Scholar: Author Only Title Only Author and Title

Feng Z, Mao Y, Xu N, Zhang B, Wei P, Yang D-L, Wang Z, Zhang Z, Zheng R, Yang L, et al (2014) Multigeneration analysis reveals the inheritance, specificity, and patterns of CRISPR/Cas-induced gene modifications in Arabidopsis. Proc Natl Acad Sci U S A 111: 4632-4637

Pubmed: Author and Title
CrossRef: Author and Title
Google Scholar: Author Only Title Only Author and Title

Friesen ML, von Wettberg EJ, Badri M, Moriuchi KS, Barhoumi F, Chang PL, Cuellar-Ortiz S, Cordeiro MA, Vu WT, Arraouadi S, et al (2014) The ecological genomic basis of salinity adaptation in Tunisian Medicago truncatula. BMC Genomics 15: 1160

Pubmed: Author and Title
CrossRef: Author and Title
Google Scholar: Author Only Title Only Author and Title

Graham PH (1992) Stress tolerance in Rhizobiaum and Bradyrhizobium, and nodulation under adverse soild conditions. Can J Microbiol 38: 475-484

Pubmed: Author and Title
CrossRef: Author and Title
Google Scholar: Author Only Title Only Author and Title

Graham PH, Rosas JC (1979) Phosphorus fertilization and symbiotic nitrogen fixation in common bean. Agron J 71:925-926

Pubmed: Author and Title
CrossRef: Author and Title
Google Scholar: Author Only Title Only Author and Title

Hernandez-Garcia CM, Bouchard R a, Rushton PJ, Jones ML, Chen X, Timko MP, Finer JJ (2010) High level transgenic expression of soybean (Glycine max) GmERF and Gmubi gene promoters isolated by a novel promoter analysis pipeline. BMC Plant Biol 10: 237

Pubmed: Author and Title
CrossRef: Author and Title
Google Scholar: Author Only Title Only Author and Title

Hindorff LA, Sethupathy P, Junkins HA, Ramos EM, Mehta JP, Collins FS, Manolio TA (2009) Potential etiologic and functional implications of genome-wide association loci for human diseases and traits. Proc Natl Acad Sci 106 : 9362-9367

Pubmed: Author and Title
CrossRef: Author and Title
Google Scholar: Author Only Title Only Author and Title

Ioannidis JPA, Thomas G, Daly MJ (2009) Validating, augmenting and refining genome-wide association signals. Nat Rev Genet 10: 318-329

Pubmed: Author and Title
CrossRef: Author and Title
Google Scholar: Author Only Title Only Author and Title

Jakobsen I (1985) The role of phosphorus in nitrogen fixation by young pea plants (Pisum sativum). Physiol Plant 64: 190-196

Pubmed: Author and Title
CrossRef: Author and Title
Google Scholar: Author Only Title Only Author and Title

Johansson ON, Fantozzi E, Fahlberg P, Nilsson AK, Buhot N, T??r M, Andersson MX (2014) Role of the penetration-resistance genes PEN1, PEN2 and PEN3 in the hypersensitive response and race-specific resistance in Arabidopsis thaliana. Plant J 79: 466-476

Pubmed: Author and Title
CrossRef: Author and Title
Google Scholar: Author Only Title Only Author and Title

Karlsson P, Christie MD, Seymour DK, Wang H, Wang X, Hagmann J, Kulcheski F, Manavella PA (2015) KH domain protein RCF3 is a tissue-biased regulator of the plant miRNA biogenesis cofactor HYL1. Proc Natl Acad Sci U S A 1-6

Pubmed: Author and Title
CrossRef: Author and Title
Google Scholar: Author Only Title Only Author and Title

Krusell L, Madsen LH, Sato S, Aubert G, Genua A, Szczyglowski K, Duc G, Kaneko T, Tabata S, de Bruijn F, et al (2002) Shoot control of root development and nodulation is mediated by a receptor-like kinase. Nature 420: 422-426

Pubmed: Author and Title
CrossRef: Author and Title
Google Scholar: Author Only Title Only Author and Title

Lang C, Long SR (2015) Transcriptomic analysis of Sinorhizobium meliloti and Medicago truncatula symbiosis using nitrogen fixation-deficient nodules. Mol Plant Microbe Interact 28: 856-68

Pubmed: Author and Title
CrossRef: Author and Title
Google Scholar: Author Only Title Only Author and Title

Larrainzar E, Riely B, Kim SC, Carrasquilla-Garcia N, Yu H-J, Hwang H-J, Oh M, Kim GB, Surendrarao A, Chasman D, et al (2015) Deep sequencing of the Medicago truncatula root transcriptome reveals a massive and early interaction between Nod factor and

ethylene signals. Plant Physiol. doi: 10.1104/pp.15.00350
Pubmed: Author and Title
CrossRef: Author and Title
Google Scholar: Author Only Title Only Author and Title

Li J-F, Norville JE, Aach J, McCormack M, Zhang D, Bush J, Church GM, Sheen J (2013) Multiplex and homologous recombination-mediated genome editing in Arabidopsis and Nicotiana benthamiana using guide RNA and Cas9. Nat Biotechnol 31: 688-91
Pubmed: Author and Title
CrossRef: Author and Title
Google Scholar: Author Only Title Only Author and Title

Lopez-Gomez M, Sandal N, Stougaard J, Boller T (2012) Interplay of flg22-induced defence responses and nodulation in Lotus japonicus. J Exp Bot 63 : 393-401
Pubmed: Author and Title
CrossRef: Author and Title
Google Scholar: Author Only Title Only Author and Title

Luo M, Gilbert B, Ayliffe M (2016) Applications of CRISPR/Cas9 technology for targeted mutagenesis, gene replacement and stacking of genes in higher plants. Plant Cell Rep 35: 1439-1450
Pubmed: Author and Title
CrossRef: Author and Title
Google Scholar: Author Only Title Only Author and Title

Mackay TFC, Stone EA, Ayroles JF (2009) The genetics of quantitative traits: challenges and prospects. Nat Rev Genet 10: 565-577
Pubmed: Author and Title
CrossRef: Author and Title
Google Scholar: Author Only Title Only Author and Title

Matejovic I (1995) Total nitrogen in plant material determined by means of dry combustion: A possible

alternative to determination by Kjedahl digestion. Commun Soil Sci Plant Anal 26: 2217-2229

Messinese E, Mun J, Yeun LH, Jayaraman D, Rougé P, Lougnon G, Schornack S, Bono J, Cook DR, Ané J (2007) A novel nuclear protein interacts with the symbiotic DMI3 Calcium- and Calmodulin- dependent protein kinase of Medicago truncatula. Mol Plant Microbe Interact 20: 912-921
Pubmed: Author and Title
CrossRef: Author and Title
Google Scholar: Author Only Title Only Author and Title

Oldroyd GED, Murray JD, Poole PS, Downie JA (2011) The rules of engagement in the legume-rhizobial symbiosis. Annu Rev Genet 45: 119-44
Pubmed: Author and Title
CrossRef: Author and Title
Google Scholar: Author Only Title Only Author and Title

Oldroyd GED, Long SR (2003) Identification and characterization of Nodulation-Signaling Pathway 2, a gene of Medicago truncatula involved in Nod Factor Signaling. Plant Physiol 131: 1027-1032
Pubmed: Author and Title
CrossRef: Author and Title
Google Scholar: Author Only Title Only Author and Title

Park BS, Seo JS, Chua N-H (2014) NITROGEN LIMITATION ADAPTATION recruits PHOSPHATE2 to target the phosphate transporter PT2 for degradation during the regulation of Arabidopsis phosphate homeostasis. Plant Cell 26: 454-464
Pubmed: Author and Title
CrossRef: Author and Title
Google Scholar: Author Only Title Only Author and Title

Pislariu CI, Murray JD, Wen J, Cosson V, Muni RRD, Wang M, Benedito V a, Andriankaja A, Cheng X, Jerez IT, et al (2012) A Medicago truncatula tobacco retrotransposon insertion mutant collection with defects in nodule development and symbiotic nitrogen fixation. Plant Physiol 159: 1686-99
Pubmed: Author and Title
CrossRef: Author and Title
Google Scholar: Author Only Title Only Author and Title

Popp C, Ott T (2011) Regulation of signal transduction and bacterial infection during root nodule symbiosis. Curr Opin Plant Biol 14: 458-467
Pubmed: Author and Title
CrossRef: Author and Title
Google Scholar: Author Only Title Only Author and Title

R Development Core Team (2013) R: A language and environment for statistical computing. R Foundation for Statistical Computing, Vienna, Austria. URL http://www.R-project.org/. R Found. Stat. Comput. Vienna, Austria.
Pubmed: Author and Title
CrossRef: Author and Title
Google Scholar: Author Only Title Only Author and Title

Ramu SK, Peng H-M, Cook DR (2002) Nod Factor induction of reactive oxygen species production is correlated with expression of the Early Nodulin gene rip1 in Medicago truncatula. Mol Plant-Microbe Interact 15: 522-528
Pubmed: Author and Title
CrossRef: Author and Title
Google Scholar: Author Only Title Only Author and Title

Rea PA (2007) Plant ATP-binding cassette transporters. Annu Rev Plant Biol 58: 347-375

Pubmed: Author and Title
CrossRef: Author and Title
Google Scholar: Author Only Title Only Author and Title

Schnabel E, Journet EP, De Carvalho-Niebel F, Duc G, Frugoli J (2005) The Medicago truncatula SUNN gene encodes a CLV1-like leucine-rich repeat receptor kinase that regulates nodule number and root length. Plant Mol Biol 58: 809-822

Pubmed: Author and Title
CrossRef: Author and Title
Google Scholar: Author Only Title Only Author and Title

Smalle J, Vierstra RD (2004) The ubiquitin 26S proteasome proteolytic pathway. Annu Rev Plant Biol 55: 555-90

Pubmed: Author and Title
CrossRef: Author and Title
Google Scholar: Author Only Title Only Author and Title

Stanton-Geddes J, Paape T, Epstein B, Briskine R, Yoder J, Mudge J, Bharti AK, Farmer AD, Zhou P, Denny R, et al (2013) Candidate genes and genetic architecture of symbiotic and agronomic traits revealed by whole-genome, sequence-based association genetics in Medicago truncatula. PLoS One 8: e65688

Pubmed: Author and Title
CrossRef: Author and Title
Google Scholar: Author Only Title Only Author and Title

Stein M, Dittgen J, Sánchez-Rodríguez C, Hou B-H, Molina A, Schulze-Lefert P, Lipka V, Somerville S (2006) Arabidopsis PEN3/PDR8, an ATP binding cassette transporter, contributes to nonhost resistance to inappropriate pathogens that enter by direct penetration. Plant Cell 18 : 731-746

Pubmed: Author and Title
CrossRef: Author and Title
Google Scholar: Author Only Title Only Author and Title

Sulieman S, Ha CV, Schulze J, Tran LS (2013) Growth and nodulation of symbiotic Medicago truncatula at different levels of phosphorus availability. J Exp Bot 64: 2701-2712

Pubmed: Author and Title
CrossRef: Author and Title
Google Scholar: Author Only Title Only Author and Title

Tadege M, Wen J, He J, Tu H, Kwak Y, Eschstruth A, Cayrel A, Endre G, Zhao PX, Chabaud M, et al (2008) Large-scale insertional mutagenesis using the Tnt1 retrotransposon in the model legume Medicago truncatula. Plant J 54: 335-347

Pubmed: Author and Title
CrossRef: Author and Title
Google Scholar: Author Only Title Only Author and Title

Tang H, Krishnakumar V, Bidwell S, Rosen B, Chan A, Zhou S, Gentzbittel L, Childs KL, Yandell M, Gundlach H, et al (2014) An improved genome release (version Mt4.0) for the model legume Medicago truncatula. BMC Genomics 15: 1-14

Pubmed: Author and Title
CrossRef: Author and Title
Google Scholar: Author Only Title Only Author and Title

Valdes-Lopez O, Arenas-Huertero C, Ramirez M, Girard L, Sanchez F, Vance CP, Luis Reyes J, Hernandez G (2008) Essential role of MYB transcription factor: PvPHR1 and microRNA: PvmiR399 in phosphorus-deficiency signalling in common bean roots. Plant Cell Environ 31: 1834-1843

Pubmed: Author and Title
CrossRef: Author and Title
Google Scholar: Author Only Title Only Author and Title

Vance CP (2001) Symbiotic nitrogen fixation and phosphorus acquisition. Plant nutrition in a world of declining renewable resources. Plant Physiol 127 : 390-397

Pubmed: Author and Title
CrossRef: Author and Title
Google Scholar: Author Only Title Only Author and Title

Veerappan V, Jani M, Kadel K, Troiani T, Gale R, Mayes T, Shulaev E, Wen J, Mysore KS, Azad RK, et al (2016) Rapid identification of causative insertions underlying Medicago truncatula Tnt1 mutants defective in symbiotic nitrogen fixation from a forward genetic screen by whole genome sequencing. BMC Genomics 1-11

Pubmed: Author and Title
CrossRef: Author and Title
Google Scholar: Author Only Title Only Author and Title

Wesley S, Helliwell C, Smith N (2001) Construct design for efficient, effective and high-throughput gene silencing in plants. Plant J 27: 581-590

Pubmed: Author and Title
CrossRef: Author and Title
Google Scholar: Author Only Title Only Author and Title

Yeaman S, Whitlock MC (2011) The genetic architecture of adaptation under migration-selection balance. Evolution 65: 1897-1911

Pubmed: Author and Title
CrossRef: Author and Title
Google Scholar: Author Only Title Only Author and Title

Young ND, Debelle F, Oldroyd GED, Geurts R, Cannon SB, Udvardi MK, Benedito VA, Mayer KF, Gouzy J, Schoof H, et al (2011)
The Medicago genome provides insight into the evolution of rhizobial symbioses. Nature 480: 520-524

Pubmed: [Author and Title](#)
CrossRef: [Author and Title](#)
Google Scholar: [Author Only](#) [Title Only](#) [Author and Title](#)